JOURNAL OF THERMOPHYSICS AND HEAT TRANSFER
Vol. 17, No. 3, July–September 2003

Natural Convective Conjugate Cooling Mechanism in Vertical Fins

C. Treviño*
Universidad Nacional Autonoma de Mexico, 04510 Mexico, D.F., Mexico
E. Luna†
Instituto Mexicano del Petróleo, 07730 Mexico, D. F., Mexico
F. Méndez‡
Universidad Nacional Autonoma de Mexico, 04510 Mexico, D.F., Mexico
and
F. J. Higuera§
Universidad Politécnica de Madrid, 28040 Madrid, Spain

An analysis is presented of the conjugate free convective heat transfer from a vertical, thermally thin fin heated from above to the surrounding fluid. An estimate is presented of the thermal penetration length over which the temperature of a very long fin would decrease from its maximum value at the top to the ambient temperature of the fluid. The solution of the problem is shown to depend on two nondimensional parameters: the Prandtl number of the fluid and the ratio s of the thermal penetration length to the actual length of the fin. The overall heat transfer rate for thermally short fins (large s) is practically independent of the fin material, whereas it depends on the thermal conductivity of the fin when s is small. Numerical and asymptotic results are given covering the whole range of s.

Nomenclature

C_p	=	specific heat of fluid
f	=	nondimensional stream function introduced in Eq. (8)
G_0	=	nondimensional temperature gradient introduced in Eq. (28)
$\tilde{G}_0$	=	nondimensional temperature gradient defined in Eq. (51)
g	=	gravity acceleration
h	=	half-thickness of the fin
L	=	length of the fin
L^*	=	thermal penetration length defined in Eq. (1)
Nu	=	Nusselt number defined in Eq. (15)
Pr	=	Prandtl number of the fluid, $\nu\rho C_p/\lambda$
Q	=	total heat flux at the top of the fin
Ra^*	=	Rayleigh number, $\rho c g \beta \Delta T L^{*3}/\lambda\nu$
Ra_h	=	Rayleigh number based on the half-thickness of the fin
Ra_L	=	Rayleigh number based on the length of the fin
s	=	ratio of L^* to L
T_0	=	temperature at the top of the fin
T_∞	=	temperature of the fluid far from the fin
U, V	=	nondimensional longitudinal and transverse velocity components, respectively, defined in Eq. (39)
x, y	=	Cartesian coordinates, longitudinal and transverse, respectively
z	=	nondimensional transverse coordinate defined in Eq. (39)
β	=	thermal expansion coefficient of fluid
ε	=	aspect ratio of the fin, h/L
η	=	nondimensional transverse coordinate defined in Eq. (8)
θ	=	nondimensional temperature of fluid defined in Eq. (8)
θ_w	=	nondimensional temperature of the fin defined in Eq. (7)
λ	=	thermal conductivity of fluid
λ_w	=	thermal conductivity of the fin
ν	=	kinematic coefficient of viscosity of fluid
ρ	=	density of fluid
σ	=	nondimensional longitudinal coordinate defined in Eq. (39)
χ	=	nondimensional longitudinal coordinate defined in Eq. (7)
ψ	=	stream function for fluid

I. Introduction

THIS paper is devoted to the study of the natural convection heat transfer from a single rectangular, nonisothermal fin to the surrounding fluid. We solve the boundary-layer equations for the fluid around the fin together with the heat conduction equation for the solid. This basic conjugated heat transfer problem has a bearing on the design and thermal control of a variety of devices, although it may be very complicated by fin-to-fin interactions in the arrays of fins typically found in heat exchangers.

The general problem of the thermal coupling between natural convection and heat conduction in vertical or horizontal surfaces has been extensively treated in the literature. Recent relevant works showing the state of the art in the analysis of these heat transfer problems include Merkin and Pop,[1] Vynnycky and Kimura,[2] and Luna et al.[3] Lock and Gunn[4] analyzed a tapered short fin in a stagnant fluid with a very large Prandtl number using a similarity formalism. In their analysis, these authors did not have to include coupling mechanism because they assumed an isothermal fin, which is reasonable for short fins with high thermal conductivity. The first analysis of the effect of a longitudinal temperature variation and the attendant longitudinal heat conduction was carried out by Sparrow and Acharya,[5] whose analysis indicates that the heat transfer coefficient is not uniform along the fin but changes with the distance to its base. Later, Kuehn et al.[6] presented a similarity solution for the conjugate

Received 29 November 2001; revision received 11 September 2002; accepted for publication 3 October 2002.

*Professor, Facultad de Cïencias.
†Researcher, Departamento de Yacimientos Naturalmente Fracturados.
‡Professor, Facultad de Ingeniería.
§Professor, Escuela Técnica Superior de Ingenieros Aeronáuticos.

free convection heat transfer from a vertical fin of infinite length, obtaining results for different values of Prandtl number. A similar study using an integral formalism was made by Himasekhar[7] for a very long fin, whereas Sarma et al.[8] studied heat-generating fins assuming prescribed velocity and temperature profiles. Recently, Mobedi et al.[9] solved the conjugate conduction–natural convection heat transfer problem for a rectangular fin attached to a partially heated horizontal base for air in laminar and steady flow.

In what follows, the conjugate natural boundary-layer problem is reformulated to obtain new solutions for nonisothermal vertical fins. We consider the case in which the base of the fin is held at a given temperature and identify a characteristic thermal penetration length L^* over which the temperature of an infinitely long fin would decay to the ambient temperature of the surrounding fluid. The ratio of L^* to the actual length L of the fin is a fundamental parameter that serves to classify the possible regimes. Other nondimensional parameters of the problem are the Prandtl number of the fluid, a Rayleigh number (to be defined precisely later), and the aspect ratio of the fin. Perturbation and numerical methods are used, together with the boundary-layer approximation for the fluid flow, to analyze the transition from a thermally short fin ($s = L^*/L \gg 1$) to a thermally long fin ($s \ll 1$) and to ascertain the influence of the thermal properties of the fin on the overall heat transfer rate. Finally, the analytical solutions obtained using perturbation techniques are compared with numerical results.

II. Orders of Magnitude

The physical problem under study is shown in Fig. 1. A vertical, downward projecting fin of length L, thickness $2h \ll L$, and infinite width is immersed in a fluid at rest far from the fin at temperature T_∞. The top of the fin is held at a temperature $T_0 = T_\infty + \Delta T > T_\infty$, thus, inducing a heat flux from the fin to the fluid that cools the fin and gives rise to an upward natural convection flow around its surface. The present study is also valid for a vertical fin whose lower base is kept at a temperature below that of the ambient fluid. Differences between the two cases may appear in the interaction of the flow with the surface to which the fin is attached, but such interaction, which may result in complex recirculating flows around corners, will not be discussed here.

Consider first an infinitely long fin. Because of the heat loss to the surrounding fluid, the temperature of the fin decreases downward from its top, decaying toward the ambient temperature of the fluid in a thermal penetration region, whose characteristic length L^* can be estimated from the balance of heat transfer to the fluid and heat conduction along the fin. When it is assumed that the Rayleigh number $Ra^* = \rho c g \beta \Delta T L^{*3}/\lambda\nu \gg 1$, where ρ, c, β, λ, and ν are the fluid density, specific heat, thermal expansion coefficient, thermal conductivity, and kinematic viscosity, respectively, the flow around the fin is confined to a natural convection boundary layer of characteristic thickness $\delta^* = (\lambda\nu L^*/\rho c g \beta \Delta T)^{1/4}$, where the characteristic velocity of the fluid is $v_c^* = (g\beta\Delta T L^* \lambda/\rho c \nu)^{1/2}$. These well-known estimates follow from the order-of-magnitude balances of vertical convection and horizontal conduction across the boundary layer ($\rho c v_c^* \Delta T/L^* = \lambda \Delta T/\delta^{*2}$) and of buoyancy and viscous forces ($g\beta\Delta T = \nu v_c^*/\delta^{*2}$). The total heat lost by conduction to the fluid per unit time and unit width of the fin is of the order of $L^*\lambda\Delta T/\delta^*$, whereas the heat conducted along the fin is of order $h\lambda_w \Delta T/L^*$, where λ_w is the thermal conductivity of the fin. The balance of these two fluxes yields

$$L^* = h\left[(\lambda_w/\lambda)^{\frac{4}{7}} \Big/ Ra_h^{\frac{1}{7}}\right] \tag{1}$$

where $Ra_h = \rho c g \beta \Delta T h^3/\lambda\nu$.

On the basis of this estimate of the thermal penetration length, finite length fins can be classified as long, if $L \gg L^*$, or short, if $L \ll L^*$. In the case $s = L^*/L \ll 1$, the actual length of the fin is largely irrelevant, and the overall Nusselt number measuring of the total heat $2Q$ evacuated by the fin per unit width and unit time is, from the previous estimates,

$$Nu_{\text{long}} = Q/\lambda\Delta T = \mathcal{O}\left(Ra^{*\frac{1}{4}}\right) = \mathcal{O}\left[(\lambda_w/\lambda)^{\frac{3}{7}} Ra_h^{\frac{1}{7}}\right] \tag{2}$$

[See Eq. (15) for a formal definition.] In the opposite case, short fins, $s \gg 1$, the longitudinal temperature variation from the top to the bottom of the fin, ΔT_{wL}, can be estimated from the energy balance $Q \sim h\lambda_w \Delta T_{wL}/L \sim L\lambda\Delta T/\delta$, where $\delta = (\lambda\nu L/\rho c g \beta \Delta T)^{1/4}$. This balance gives

$$\Delta T_{wL}/\Delta T \sim (\lambda/\lambda_w)(L^2/h\delta) \sim \left(1\Big/s^{\frac{7}{4}}\right) \ll 1 \tag{3}$$

which means that the temperature of the fin is almost uniform and equal to its top temperature for values of s large compared with unity. The overall Nusselt number in this regime is

$$Nu_{\text{short}} = Q/\lambda\Delta T = \mathcal{O}\left(Ra^{*\frac{1}{4}} \Big/ s^{\frac{3}{4}}\right) \tag{4}$$

Finally, the temperature variation across the fin must be estimated to ascertain the conditions of validity of the thermally thin-fin approximation, which will be used in what follows. With ΔT_{wh} the characteristic temperature variation across the fin, the condition that the heat flux entering the fluid should come from the solid implies that $\lambda\Delta T/\delta \sim \lambda_w \Delta T_{wh}/h$, or with use of the earlier estimate of δ,

$$(\Delta T_{wh}/\Delta T) \sim (\lambda/\lambda_w)^{\frac{8}{7}} Ra_h^{\frac{2}{7}} \sim (h/L^*)^2 \tag{5}$$

for all but very short fins. Therefore, the thermally thin approximation ($\Delta T_{wh} \ll \Delta T$) can be used if the thermal conductivity of the fin satisfies $\lambda_w \gg \lambda Ra_h^{1/4}$. Within this approximation, the temperature of the fin depends only on the distance x along the fin, and the local energy balance for the fin reads

$$h\lambda_w \frac{d^2 T_w}{dx^2} = -\lambda \left.\frac{\partial T}{\partial y}\right|_{y=0} \tag{6}$$

where $T(x, y)$ denotes the temperature of the fluid and the derivative on the right-hand side is evaluated in the fluid at the surface of the fin.

III. Formulation

The heat transfer problem can be studied using the nondimensional variables

$$\chi = \frac{x}{L}, \qquad \theta_w = \frac{T_w(x) - T_\infty}{T_0 - T_\infty} \tag{7}$$

$$\eta = \frac{Ra_L^{\frac{1}{4}} y}{L\chi^{\frac{1}{4}}}, \qquad f(\chi, \eta) = \frac{\psi Pr}{\nu Ra_L^{\frac{1}{4}} \chi^{\frac{3}{4}}}, \qquad \theta = \frac{T(x, y) - T_\infty}{T_0 - T_\infty} \tag{8}$$

where x and y are the vertical and horizontal distances defined in Fig. 1 and ψ is the stream function of the fluid defined in the usual manner. In nondimensional variables, Eq. (6) becomes

$$s^{\frac{7}{4}} \frac{d^2\theta_w}{d\chi^2} = -\frac{1}{\chi^{\frac{1}{4}}} \left.\frac{\partial\theta}{\partial\eta}\right|_{y=0} \tag{9}$$

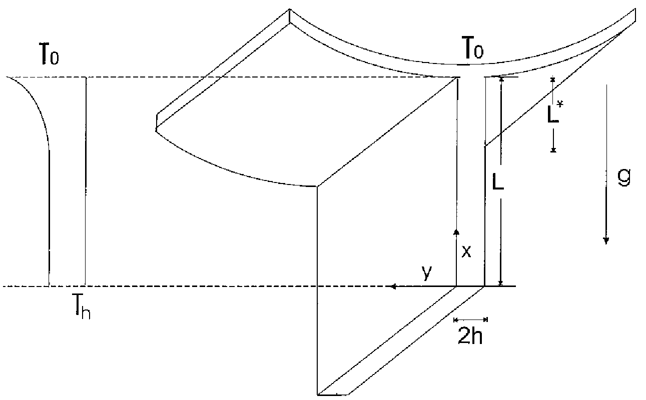

Fig. 1 Schematic diagram of the physical model.

and the boundary conditions at the top and bottom of the fin are

$$\theta_w = 1, \qquad \frac{\mathrm{d}\theta_w}{\mathrm{d}\chi} = 0 \tag{10}$$

at $\chi = 1$ and 0, respectively.

The nondimensional longitudinal momentum and energy equations for the fluid in the boundary layer are

$$\frac{\partial^3 f}{\partial \eta^3} + \theta = \frac{1}{Pr}\left\{\frac{1}{2}\left(\frac{\partial f}{\partial \eta}\right)^2 - \frac{3}{4} f \frac{\partial^2 f}{\partial \eta^2} + \chi\left[\frac{\partial f}{\partial \eta}\frac{\partial^2 f}{\partial \chi \partial \eta} - \frac{\partial f}{\partial \chi}\frac{\partial^2 f}{\partial \eta^2}\right]\right\} \tag{11}$$

$$\frac{\partial^2 \theta}{\partial \eta^2} + \frac{3}{4} f \frac{\partial \theta}{\partial \eta} = \chi\left[\frac{\partial f}{\partial \eta}\frac{\partial \theta}{\partial \chi} - \frac{\partial f}{\partial \chi}\frac{\partial \theta}{\partial \eta}\right] \tag{12}$$

where the Boussinesq approximation has been used. The boundary conditions for these equations at $\eta = 0$ are

$$f = \frac{\partial f}{\partial \eta} = 0, \qquad \theta = \theta_w \tag{13}$$

and for $\eta \to \infty$

$$\frac{\partial f}{\partial \eta} = \theta = 0 \tag{14}$$

plus conditions of regularity at the origin of the boundary layer $\chi = 0$.

The solution of problems (9–14) should determine

$$\theta_w = F(\chi; s, Pr)$$

The thermal performance of the fin can be evaluated by means of a nondimensional global heat flux (Nusselt number) defined as

$$Nu = \frac{Q}{\lambda(T_\infty - T_0)} = sRa^{*\frac{1}{4}} \left.\frac{\mathrm{d}\theta_w}{\mathrm{d}\chi}\right|_{\chi=1} \quad \text{where} \quad Q = h\lambda_w \left.\frac{\mathrm{d}T_w}{\mathrm{d}x}\right|_L \tag{15}$$

IV. Numerical Method and Results

The problem [Eqs. (9–14)] has been solved numerically for different values of the parameters s and Prandtl number. Equation for the nondimensional fin temperature is handled by means of a pseudotransient procedure that amounts to rewriting Eq. (9) in the form

$$\frac{\partial \theta_w}{\partial \tau} = s^{\frac{7}{4}} \chi^{\frac{1}{4}} \frac{\partial^2 \theta_w}{\partial \chi^2} + \left.\frac{\partial \theta}{\partial \eta}\right|_0 \tag{16}$$

and marching in artificial time τ until a steady state is attained. The nondimensional heat flux $(\partial\theta/\partial\eta)_0$ is obtained at each time step in terms of the instantaneous temperature distribution of the fin by solving the boundary-layer equations for the fluid [Eqs. (11–14)] with a standard finite difference method and a quasi-linearization technique.

The boundary conditions in the fluid for $\eta \to \infty$ were imposed at a finite distance η_∞, chosen from numerical experiments in which η_∞ is increased until its value ceases to affect the solution. (For $Pr = 1$, we find that $\eta_\infty = 9$ produces an error in the solution less than 1×10^{-10}.) The solution of the governing equations for the case of $Pr \to \infty$ was obtained using the boundary condition $\partial^2 f/\partial \eta^2 = 0$ instead of $\partial f/\partial \eta = 0$ at $\eta = \eta_\infty$. The mesh used for the balance equations was 200×200.

Figure 2 shows the nondimensional temperature of the fin as a function of the nondimensional longitudinal coordinate χ for $Pr = 1$ and different values of s. The temperature of the fin is almost uniform for very large values of s. As the value of s decreases (increasing L), the temperature of the lower base of the fin decreases. The thermally long fin regime is clearly valid for $s \leq 0.075$. The overall reduced Nusselt number, $Nu/Ra^{*1/4}$, is given as a function of s in Figs. 3 and 4, for Prandtl numbers of 10 and 0.72, respectively. Figures 3 and 4 include numerical and asymptotic results for short and long fins to be discussed in the following sections; compare Eqs. (38) and (51). They display the full transition from a thermally short to a thermally long fin.

To clarify the influence of the fin material in the overall heat transfer rate, we present the Nusselt number for three different vertical thin metallic fins (steel, aluminum, and copper) in air with an

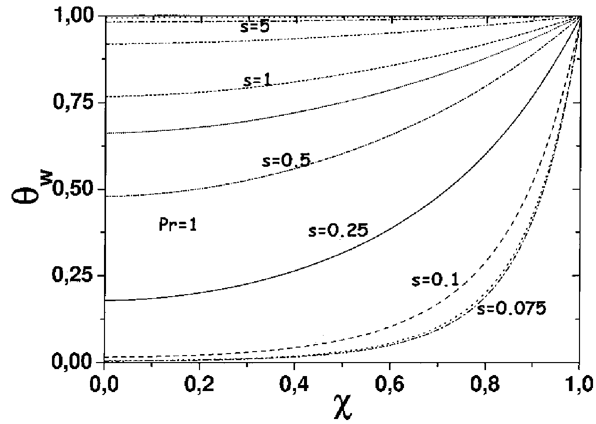

Fig. 2 Nondimensional temperature profiles obtained numerically as functions of the nondimensional longitudinal coordinate for different values of *s* and *Pr* = 1.

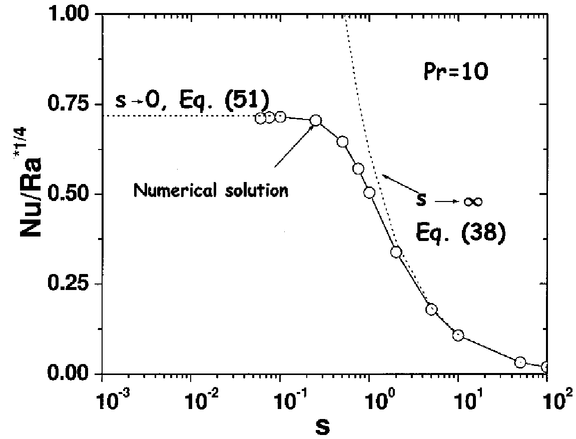

Fig. 3 Reduced Nusselt number, $Nu/Ra^{*1/4}$, as a function of *s* for *Pr* = 10, numerical and asymptotic results.

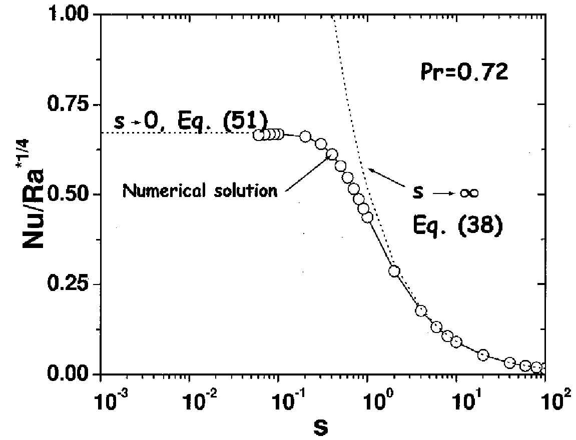

Fig. 4 Reduced Nusselt number, $Nu/Ra^{*1/4}$, as a function of *s* for *Pr* = 0.72 (air), numerical and asymptotic results.

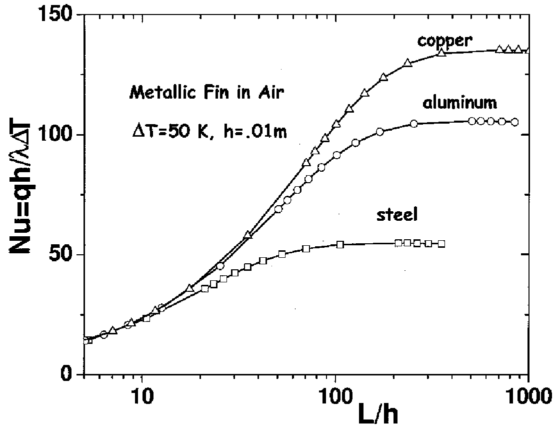

Fig. 5 Nusselt number at bottom of fin as a function of inverse of aspect ratio *L/h* for three different metallic materials of the fin immersed in air at room temperature; ΔT = 50 K and *h* = 0.01 m.

overall temperature difference of 50 K and a half-thickness of 1 cm in Fig. 5. The overall Nusselt number is plotted as a function of the inverse of the aspect ratio of the fin (L/h). The thermal conductivity of the fin material has a little influence on the overall heat transfer rate for $L/h \lesssim 10$, whereas a strong influence of the metal used is apparent for $L/h \gtrsim 10$. The Nusselt number is independent of the length of the fin once saturation is reached ($L \sim 10h$).

V. Short Fins

An asymptotic solution of problem [Eqs. (9–14)] for large values of s can be sought as a regular expansion in powers of $s^{-7/4}$, which is the small parameter dictated by the relationship (3). The solution can then be written as

$$\begin{Bmatrix}\theta_w\\ \theta\\ f\end{Bmatrix} = \begin{Bmatrix}\theta_{w0}\\ \theta_0(\eta)\\ f_0(\eta)\end{Bmatrix} + \sum_{j=1}^{\infty}\frac{1}{s^{7j/4}}\begin{Bmatrix}\theta_{wj}(\chi)\\ \theta_j(\chi,\eta)\\ f_j(\chi,\eta)\end{Bmatrix} \tag{17}$$

Carrying these expansions into the nondimensional equations (9), (11), and (12), and the boundary conditions, and keeping terms up to order $s^{-7/2}$ for the solid and up to order $s^{-7/4}$ in the fluid, we obtain the following set of equations.

For the solid,

$$\frac{\mathrm{d}^2\theta_{w0}}{\mathrm{d}\chi^2} = 0 \tag{18}$$

for $j \geq 1$,

$$\frac{\mathrm{d}^2\theta_{wj}}{\mathrm{d}\chi^2} = -\frac{1}{\chi^{\frac{1}{4}}}\frac{\partial\theta_{j-1}}{\partial\eta}\bigg|_{\eta=0} \tag{19}$$

with the boundary conditions, for $j = 0, 1, \ldots,$

$$\frac{\mathrm{d}\theta_{wj}(0)}{\mathrm{d}\chi} = 0 \tag{20}$$

where, for $j = 1, \ldots,$

$$\theta_{w0}(1) - 1 = \theta_{wj}(1) = 0 \tag{21}$$

For the fluid,

$$\frac{\mathrm{d}^3 f_0}{\mathrm{d}\eta^3} + \theta_0 - \frac{1}{Pr}\left\{\frac{1}{2}\left(\frac{\mathrm{d}f_0}{\mathrm{d}\eta}\right)^2 - \frac{3}{4}f_0\frac{\mathrm{d}^2 f_0}{\mathrm{d}\eta^2}\right\} = 0 \tag{22}$$

$$\frac{\mathrm{d}^2\theta_0}{\mathrm{d}\eta^2} + \frac{3}{4}f_0\frac{\mathrm{d}\theta_0}{\mathrm{d}\eta} = 0 \tag{23}$$

$$\frac{\partial^3 f_1}{\partial\eta^3} + \theta_1 = \frac{1}{Pr}\left(\frac{\mathrm{d}f_0}{\mathrm{d}\eta}\frac{\partial f_1}{\partial\eta} - \frac{3}{4}f_0\frac{\partial^2 f_1}{\partial\eta^2} - \frac{3}{4}\frac{\mathrm{d}^2 f_0}{\mathrm{d}\eta^2}f_1\right) + \frac{1}{Pr}\chi\left[\frac{\mathrm{d}f_0}{\mathrm{d}\eta}\frac{\partial^2 f_1}{\partial\chi\partial\eta} - \frac{\mathrm{d}^2 f_0}{\mathrm{d}\eta^2}\frac{\partial f_1}{\partial\chi}\right] \tag{24}$$

$$\frac{\partial^2\theta_1}{\partial\eta^2} + \frac{3}{4}f_0\frac{\partial\theta_1}{\partial\eta} + \frac{3}{4}\frac{\mathrm{d}\theta_0}{\mathrm{d}\eta}f_1 = \chi\left[\frac{\mathrm{d}f_0}{\mathrm{d}\eta}\frac{\partial\theta_1}{\partial\chi} - \frac{\mathrm{d}\theta_0}{\mathrm{d}\eta}\frac{\partial f_1}{\partial\chi}\right] \tag{25}$$

etc., with the boundary conditions, at $\eta = 0$, for $j = 0, 1, \ldots,$

$$f_j = \frac{\partial f_j}{\partial\eta} = 0, \qquad \theta_0 = \theta_{w0}, \qquad \theta_1 = \theta_{w1}, \ldots \tag{26}$$

and for $\eta \to \infty$, for $j = 0, 1, \ldots,$

$$\frac{\partial f_j}{\partial\eta} = \theta_j = 0 \tag{27}$$

The solution of Eq. (18) with the boundary conditions (20) and (21) is $\theta_{w0} = 1$. When this result is used, the leading-order problem for the fluid coincides with the classical problem of a boundary layer on a uniform temperature surface, whose solution can be found elsewhere.[10] In particular, the nondimensional temperature gradient at the wall is given by[10]

$$\frac{\mathrm{d}\theta_0}{\mathrm{d}\eta}\bigg|_{\eta=0} = -G_0(Pr) \approx -\frac{3}{4}\left[\frac{2Pr}{5\left(1 + 2Pr^{\frac{1}{2}} + 2Pr\right)}\right]^{\frac{1}{4}} \tag{28}$$

Thus, we can obtain the temperature gradient at the surface of the fin needed to evaluate the right-hand side of Eq. (19) for $j = 1$. This equation can be integrated twice to yield

$$\theta_{w1} = \sum_{n=0,\frac{7}{4}} a_n\chi^n = -\frac{16}{21}G_0(Pr)\left(1 - \chi^{\frac{7}{4}}\right) \tag{29}$$

Here $a_0 = -a_{7/4} = -16G_0(Pr)/21$. The solutions to the linear Eqs. (24) and (25) are of the form

$$f_1(\chi,\eta) = \sum_{n=0,\frac{7}{4}} a_n\chi^n g_n(\eta, Pr)$$

$$\theta_1(\chi,\eta) = \sum_{n=0,\frac{7}{4}} a_n\chi^n\varphi_n(\eta, Pr) \tag{30}$$

where φ_n and g_n are the solutions of the linear ordinary differential equations,

$$\frac{\mathrm{d}^3 g_n}{\mathrm{d}\eta^3} + \varphi_n + \frac{1}{Pr}\left\{-\frac{\mathrm{d}f_0}{\mathrm{d}\eta}\frac{\mathrm{d}g_n}{\mathrm{d}\eta} + \frac{3}{4}g_n\frac{\mathrm{d}^2 f_0}{\mathrm{d}\eta^2} + \frac{3}{4}f_0\frac{\mathrm{d}^2 g_n}{\mathrm{d}\eta^2}\right. \tag{31}$$

$$\left. -n\left[\frac{\mathrm{d}f_0}{\mathrm{d}\eta}\frac{\mathrm{d}g_n}{\mathrm{d}\eta} - g_n\frac{\mathrm{d}^2 f_0}{\mathrm{d}\eta^2}\right]\right\} = 0 \tag{32}$$

$$\frac{\mathrm{d}^2\varphi_n}{\mathrm{d}\eta^2} + \frac{3}{4}f_0\frac{\mathrm{d}\varphi_n}{\mathrm{d}\eta} + \frac{3}{4}g_n\frac{\mathrm{d}\theta_0}{\mathrm{d}\eta} - n\left[\frac{\mathrm{d}f_0}{\mathrm{d}\eta}\varphi_n - g_n\frac{\mathrm{d}\theta_0}{\mathrm{d}\eta}\right] = 0 \tag{33}$$

with the boundary conditions

$$g_n = \frac{\mathrm{d}g_n}{\mathrm{d}\eta} = \varphi_n - 1 = 0, \qquad \frac{\mathrm{d}g_n}{\mathrm{d}\eta} = \varphi_n = 0 \tag{34}$$

at $\eta = 0$ and for $\eta \to \infty$, respectively.

Figure 6 shows $G_0(Pr)$ and $G_1(n, Pr) = -\mathrm{d}\varphi_n/\mathrm{d}\eta|_{\eta=0}$ for $n = 0$ and $\frac{7}{4}$, as functions of the Prandtl number. Using the invariance properties of the boundary-layer equations, we obtain that $G_1(0, Pr) = 5/4G_0(Pr)$. Therefore, the first-order temperature gradient at the fluid is given by

$$\frac{\partial\theta_1}{\partial\eta}\bigg|_{\eta=0} = \frac{20}{21}G_0^2(Pr) - \frac{16}{21}G_0(Pr)G_1\left(\frac{7}{4}, Pr\right)\chi^{\frac{7}{4}} \tag{35}$$

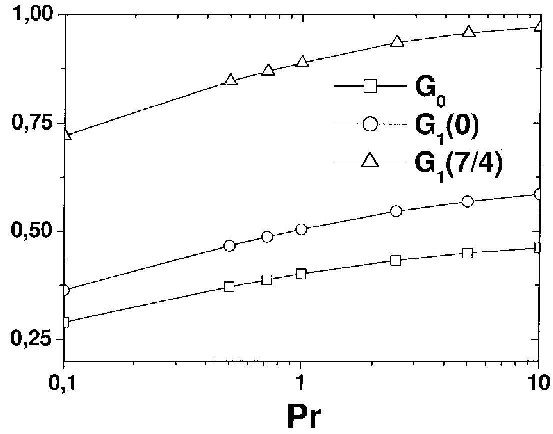

Fig. 6 Nondimensional temperature gradients $G_0(Pr)$, $G_1(0, Pr)$, and $G_1(7/4, Pr)$ as functions of the Prandtl number for a thermally short fin.

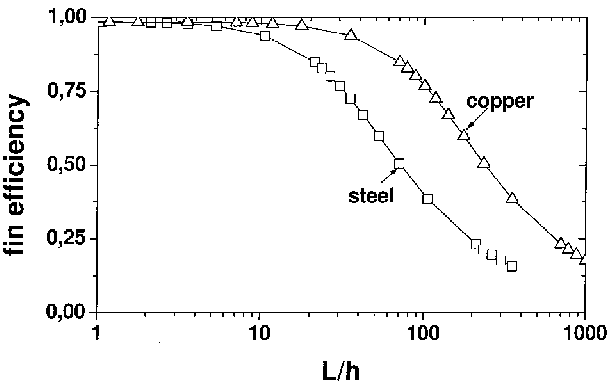

Fig. 7 Fin efficiency as a function of the inverse of aspect ratio *L/h* for two different metallic materials of the fin immersed in air at room temperature.

Using the same procedure for θ_{w2}, we obtain

$$\theta_{w2} = (16/21)G_0(Pr)\Big[(20/21)G_0(Pr)\big(1 - \chi^{\frac{7}{4}}\big) - (4/35)G_1\big((7/4), Pr\big)\big(1 - \chi^{\frac{7}{2}}\big)\Big] \tag{36}$$

In summary, the nondimensional temperature of the plate for large values of the parameter s can be written as

$$\theta_w = 1 - \big(16\big/21s^{\frac{7}{4}}\big)G_0(Pr)\big(1 - \chi^{\frac{7}{4}}\big) + \big(16\big/21s^{\frac{14}{4}}\big)G_0(Pr) \times \Big[(20/21)G_0(Pr)\big(1 - \chi^{\frac{7}{4}}\big) - (4/35)G_1(7/4, Pr)\big(1 - \chi^{\frac{7}{2}}\big)\Big] + \mathcal{O}\big(s^{-\frac{21}{4}}\big) \tag{37}$$

The reduced Nusselt number defined in Eq. (15) is then

$$Nu\Big/Ra^{*\frac{1}{4}} = (4/3)\big[G_0(Pr)\big/s^{\frac{3}{4}}\big]\Big\{1 - (20/21)\big[G_0(Pr)\big/s^{\frac{7}{4}}\big] + (8/35)\big[G_1(7/4, Pr)\big/s^{\frac{7}{4}}\big]\Big\} + \mathcal{O}\big(s^{-\frac{17}{4}}\big) \tag{38}$$

where the leading term is the overall Nusselt number for an isothermal fin. The thermal properties of the material, entering through the definition of L^*, play no role in the heat transfer at this leading order because $Ra^{*^{1/4}}/s^{3/4} = Ra_L^{1/4}$ is independent of L^*. The two-term approximation (38) turns out to give very good results even for values of s of order unity.

The thermal efficiency of a fin is often defined in the literature as the ratio of the heat transfer rate of the actual fin to the heat transfer rate that would be obtained if the temperature of the fin were uniform. Figure 7 shows the thermal efficiency of the fin as a function of L/h for fins of steel and copper. As can be seen, the thermal efficiency decreases as the overall heat flux increases, which makes the definition of doubtful usefulness. Perhaps a better measure of the fin performance could be given by the ratio of the actual heat transfer rate to the heat transfer rate that would be obtained in the absence of any fin. When it is assumed that the fin is attached to a circular tube of diameter D, the heat flux at the wall of the tube can be written as[11] $Nu = C(Pr)(h/D)^{1-3m}Ra_h^m$, where $C = 0.402$ for $Pr = 0.72$ and $m = \frac{1}{4}$. For a tube diameter of $D = 15$ cm, Fig. 8 shows the thermal fin performances as a function of L/h for two different fin materials. A slightly different definition of the efficiency kindly suggested by a reviewer is loss from the fin minus loss from the wall divided by loss from the wall.

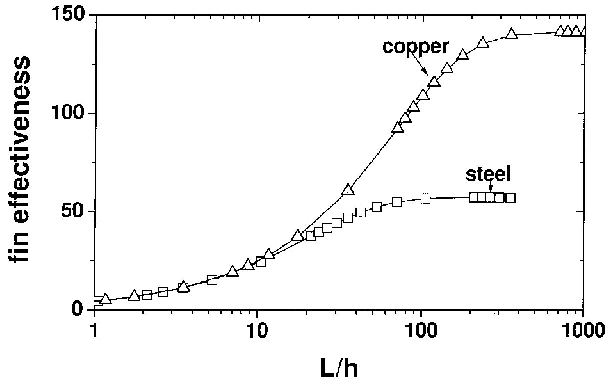

Fig. 8 Fin effectiveness as a function of the inverse of aspect ratio *L/h* for two different metallic materials of the fin immersed in air at room temperature.

VI. Long Fins

To analyze the asymptotic limit of long fins ($s \ll 1$), it is convenient to rewrite the problem in terms of the variables

$$\sigma = (L - x)/L^*, \qquad z = (y/L^*)Ra^{*\frac{1}{4}}$$

$$U = \Big(L^*Pr\Big/\nu Ra^{*\frac{1}{2}}\Big)u, \qquad V = \Big(L^*Pr\Big/\nu Ra^{*\frac{1}{4}}\Big)v \tag{39}$$

Here, σ is the nondimensional distance measured downward from the top of the fin and u is the vertical velocity of the fluid, measured positive downward. The nondimensional governing equations are

$$\frac{\partial U}{\partial \sigma} + \frac{\partial V}{\partial z} = 0 \tag{40}$$

$$\frac{\partial^2 U}{\partial z^2} - \theta = \frac{1}{Pr}\left(U\frac{\partial U}{\partial \sigma} + V\frac{\partial U}{\partial z}\right) \tag{41}$$

$$U\frac{\partial \theta}{\partial \sigma} + V\frac{\partial \theta}{\partial z} = \frac{\partial^2 \theta}{\partial z^2} \tag{42}$$

$$\frac{d\theta_w^2}{d\sigma^2} = -\frac{\partial \theta}{\partial z}\bigg|_{z=0} \tag{43}$$

to be solved with the boundary conditions, at $z = 0$,

$$U = V = \theta - \theta_w = 0 \tag{44}$$

for $z \to \infty$,

$$U = \theta = 0 \tag{45}$$

where

$$\theta_w = 1, \qquad \theta_w = 0 \tag{46}$$

at $\sigma = 0$ and for $\sigma \to \infty$, respectively.

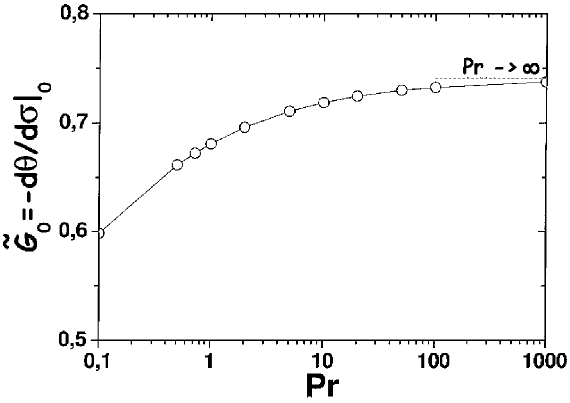

Fig. 9 Nondimensional temperature gradient $\tilde{G}_0(Pr)$ as a function of Prandtl number for a thermally long fin and asymptotic values for large and small values of the Prandtl numbers.

This problem has a self-similar solution of the form

$$\theta = \theta_w(\sigma)\phi(\xi), \qquad U = \frac{7^{\frac{1}{2}}}{\tilde{G}_0^{\frac{1}{2}}}\theta_w^{\frac{3}{7}}(\sigma)\frac{\mathrm{d}h}{\mathrm{d}\xi}, \qquad \xi = \frac{\tilde{G}_0^{\frac{1}{4}}}{7^{\frac{1}{4}}}z\theta_w^{\frac{2}{7}}(\sigma) \tag{47}$$

where $\theta_w = (1 + \tilde{G}_0\sigma/7)^{-7}$. Here the constant $\tilde{G}_0$ represents the nondimensional heat flux, or reduced Nusselt number $Nu/Ra^{*^{1/4}} = -\mathrm{d}\theta_w/\mathrm{d}\sigma|_0$, which is to be determined as part of the solution. The functions $\phi(\xi)$ and $h(\xi)$ satisfy the ordinary differential equations

$$\frac{\mathrm{d}^3h}{\mathrm{d}\xi^3} - \phi = \frac{1}{Pr}\left[h\frac{\mathrm{d}^2h}{\mathrm{d}\xi^2} - 3\left(\frac{\mathrm{d}h}{\mathrm{d}\xi}\right)^2\right] \tag{48}$$

$$\frac{\mathrm{d}^2\phi}{\mathrm{d}\xi^2} = \left[h\frac{\mathrm{d}\phi}{\mathrm{d}\xi} - 7\phi\frac{\mathrm{d}h}{\mathrm{d}\xi}\right] \tag{49}$$

with the conditions

$$h(0) = \left.\frac{\mathrm{d}h}{\mathrm{d}\xi}\right|_{\xi=0} = \phi(0) - 1 = \left.\frac{\mathrm{d}h}{\mathrm{d}\xi}\right|_{\xi\to\infty} = \phi(\infty) = 0 \tag{50}$$

The solution of Eqs. (48–50), which do not contain $\tilde{G}_0$, determines $\mathrm{d}\phi/\mathrm{d}\xi|_{\xi=0}$ as a function of the Prandtl number. Then $\partial\theta/\partial z|_{z=0} = (\theta_w^{9/7}\tilde{G}_0^{1/4}/7^{1/4})\,\mathrm{d}\phi/\mathrm{d}\xi|_{\xi=0}$, and carrying this result into (43), we obtain

$$\frac{Nu}{Ra^{*\frac{1}{4}}} = \tilde{G}_0(Pr) = \frac{7^{\frac{3}{7}}}{8^{\frac{4}{7}}}\left(-\left.\frac{\mathrm{d}\phi}{\mathrm{d}\xi}\right|_{\xi=0}\right)^{\frac{4}{7}} \tag{51}$$

This $\tilde{G}_0(Pr)$ is plotted in Fig. 9. For very large values of the Prandtl number $\tilde{G}_0(\infty) \doteq 0.7412\ldots$, whereas for very small Prandtl numbers $\tilde{G}_0(Pr \to 0) \sim 0.979Pr^{1/7}$.

VII. Conclusions

An analytical and numerical study has been carried out of the conjugated heat transfer in a vertical thermally thin fin with a prescribed temperature at its top. For large values of the Rayleigh number, the problem is shown to depend on two nondimensional parameters: $s = L^*/L$ and Prandtl number Pr. The limiting regimes of thermally long and thermally short fins are defined and analyzed using asymptotic techniques. For large values of s (thermally short fins), the total heat flux depends only weakly on the thermal properties of the fin material, as given by the first term in Eq. (38). The leading-order behavior is in fact independent of the thermal conductivity of the fin. A two-term asymptotic solution is derived for the limit of $s \to \infty$. On the other hand, the problem has a self-similar closed-form solution for small values of s (thermally long fins), yielding an overall Nusselt number strongly dependent on the thermal conductivity of the fin material and the thickness of the fin. The transition from short fins (low heat transfer rates) to long fins (large heat transfer rates) has been studied using numerical techniques.

References

[1]Nomura, S., Thomas, K. M., Merkin, J. H., and Pop, I., "Conjugate Free Convection on a Vertical Plate," *International Journal of Heat and Mass Transfer*, Vol. 39, No. 7, 1996, pp. 1527–1534.

[2]Kotelnikov, V. A., Persits, I. E., Surin, N. N., Danilevskaya, L. B., Sekiguchi, H., Bui, C., Vynnycky, M., and Kimura, S., "Conjugate Free Convection Due to a Heated Vertical Plate," *International Journal of Heat and Mass Transfer*, Vol. 39, No. 5, 1996, pp. 1067–1080.

[3]Luna, E., Treviño, C., and Higuera, F. J., "Conjugate Natural Convection Heat Transfer Between Two Fluids Separated by an Horizontal Wall: Steady-State Analysis," *Heat and Mass Transfer*, Vol. 31, 1996, pp. 353–358.

[4]Lock, G. S. H., and Gunn, J. C., "Laminar Free Convection from a Downward-Projecting Fin," *Journal of Heat Transfer*, Vol. 90, No. 1, 1968, pp. 63–70.

[5]Sparrow, E. M., and Acharya, S., "A Natural Convection Fin with a Solution-Determined Nonmonotonically Varying Heat Transfer Coefficient," *Journal of Heat Transfer*, Vol. 103, No. 3, 1981, pp. 218–225.

[6]Kuehn, T. H., Kwon, S. S., and Tolpadi, A. K., "Similarity Solution for Conjugate Natural Convection Heat Transfer from a Long Vertical Plate Fin," *International Journal of Heat and Mass Transfer*, Vol. 26, No. 11, 1983, pp. 1718–1721.

[7]Himasekhar, K., "Integral Analysis of Conjugate Natural Convection Heat Transfer from a Long Vertical Fin," *International Journal of Heat and Mass Transfer*, Vol. 30, No. 1, 1987, pp. 201–203.

[8]Sarma, P. K., Subrahmanyam, T., and Dharma Rao, V., "Natural Convection from a Vertical Heat-Generating Fin—A Conjugate Problem," *Journal of Heat Transfer*, Vol. 110, No. 1, 1988, pp. 99–102.

[9]Mobedi, M., Saidi, A., and Sunden, B., "Computation of Conjugate Natural Convection Heat Transfer from a Rectangular Fin on a Partially Heated Horizontal Base," *Heat and Mass Transfer*, Vol. 33, 1998, pp. 333–336.

[10]Kays, W. M., and Crawford, M. E., *Convective Heat and Mass Transfer*, McGraw–Hill, New York, 1980, p. 318.

[11]Gebhart, Y., Jaluria, R. L., Mahajan, B., and Sammakia, B., *Buoyancy-Induced Flows and Transport*, Springer, Berlin, 1988, p. 202.